Prediction of grain size evolution during thermal treatments at the mesoscopic scale: numerical improvements and industrial examples

A. Settefrati[1,a*], B. Scholtes[1,2,b], N. Bozzolo[2,c], E. Perchat[1,d], M. Bernacki[2,e]

[1]Transvalor S.A., Parc de Haute Technologie – Sophia Antipolis, 694 avenue du Docteur Maurice Donat, 06250 Mougins, France

[2]Mines ParisTech, PSL Research University, CEMEF Centre de mise en forme des matériaux, CNRS UMR 7635, CS 10207 rue Claude Daunesse, 06904 Sophia Antipolis Cedex, France

[a]amico.settefrati@transvalor.com, [b]benjamin.scholtes@mines-paristech.fr, [c]nathalie.bozzolo@mines-paristech.fr, [d]etienne.perchat@transvalor.com, [e]marc.bernacki@mines-paristech.fr

Abstract. Recently, an original full field model working at the mesoscopic scale using the level set (LS) method in a finite element (FE) framework has been introduced. This approach has demonstrated its potential for the simulation of grain growth and recrystallization problems. Through the development of the DIGIMU® software, this methodology is now considered for industrial applications. The paper presents (i) the recent developments made on the LS approach and (ii) some examples of large scale simulations in two and three dimensions considering thermal treatments applied on materials. Grain boundaries motion considering the presence or not of second phase particles (like precipitates) are investigated.

Introduction

Mechanical and functional properties of metallic materials are strongly related to their microstructures, which are themselves inherited from thermal and mechanical processing. A precise control of the grain size evolution during these thermomechanical and thermal treatments is one of the key factors for reaching the required final in-use material properties, particularly for the aerospace and nuclear industries. An accurate prediction of the grain size is thus of prime importance. The goal is to correctly describe the main physical mechanisms occurring in metals i.e. grain boundary (GB) migration, work-hardening, recovery, nucleation and grain growth related to dynamic, static or metadynamic recrystallization.

Macroscopic and homogenized metallurgical models are widely used, mainly due to their low computational cost [1, 2]. If this mean field framework is quite convenient, it can be synonymous for a given material of a large amount of experiments with advanced laboratory devices. Moreover, the homogenization of the microstructure does not permit to capture some very local phenomena. In order to overcome these issues, lower-scale models (called full field models) have been developed over the last decades with the aim to simulate explicitly the microstructural evolution [3-5]. The idea behind these "mesoscale" simulations is that the morphology and the topology of the GB network play a non-negligible role in the evolution of the microstructure. In these approaches, simulations are performed on Representative Volume Elements (RVEs) where the microstructural features are explicitly represented. Boundary conditions applied to the RVE are representative of what suffered a material point at the macroscopic scale (thermal or thermomechanical cycle).

Recently a new full field approach, based on a LS description of the interfaces in a FE context has been introduced to model primary recrystallization, including the nucleation stage, and has been extended to take into account the grain growth stage of monophasic polycrystalline structures [6-8]. Moreover in this LS context, Smith-Zener pinning (SZP) phenomenon can be taken into account in a natural way [9]. Modelling at the mesoscopic scale can thus be a help for understanding complex microstructural phenomena such as abnormal grain growth; it can also be used to optimize/calibrate higher scale models through numerical experiments leading to a real multiscale approach. Full field models are generally associated with high computation times. Recent major developments and improvements made on the LS approach [10, 11] make possible its use in an industrial context. After introducing the FE-LS numerical model in the next section, some examples of large scale simulations in 2D and 3D are presented. This paper focuses on thermal treatments.

Numerical model description

Level Set (LS) function. The microstructural evolution is given by the displacement of interfaces (grain boundaries for example). The model considered here works around a LS description of the interfaces in a FE framework. This method has the advantage of avoiding the difficult problem of tracking interfaces. Indeed a LS function ψ is defined over a domain Ω as the signed distance function to the interface of a sub-domain G of Ω. The values of ψ are calculated at each mesh node and the sign is defined as positive inside G and negative outside:

$$\forall t \begin{cases} \psi(x,t) = \pm d\big(x, \Gamma(t)\big), x \in \Omega \\ \Gamma(t) = \{x \in \Omega, \psi(x,t) = 0\} \end{cases} \tag{1}$$

where $d(.,.)$ corresponds to the Euclidean distance. The interface is implicitly given by the level 0 of the function ψ.

Theoretically, each grain of a polycrystal must be represented by its own LS function. In practice, non-neighbouring grains in the initial microstructure (separated by a certain number of grains) can be grouped to form global LS (GLS) functions. This approach allows using a small number of functions Np compared to the total number of grains constituting the microstructure Ng and thus limits the numerical cost. The interface of each GLS function is then displaced by solving a set of convective-diffusive equations [7]:

$$\forall p \in \{1, \dots, N_p\}: \begin{cases} \frac{\partial \psi_p(x,t)}{\partial t} - m\gamma\Delta\psi_p(x,t) + v_e.\nabla\psi_p(x,t) = 0, \\ \psi_p(x, t = 0) = \psi_p^0(x) \end{cases} \tag{2}$$

where m and γ are respectively the GB mobility and energy. The diffusive term refers to capillarity effects while the convective one is related to stored energy gradients throughout the microstructure.

Reinitialisation procedure. The distance function must be reinitialized at each time step in order to keep the metric property $\|\nabla\psi_p\| = 1$ during all the simulation. Indeed, even if reinitialization is favourable for the regularity of the LS function, this treatment is especially crucial in order to verify that the capillarity effects are properly described by the diffusive part of Eq. (2). The classical approach used in [7-9] consists in solving a Hamilton-Jacobi (HJ) equation for each GLS function. This method corrects iteratively the LS functions until their respective metric properties are restored. Based on the resolution of a large number of partial differential equations systems, the HJ method can require a lot of iterations for achieving convergence. An efficient and parallel reinitialization algorithm based on a direct approach and using optimized searching procedures has been recently developed [10]. Based on the exact analytic reconstruction of the distance function, this method leads to significant computational cost reductions.

Recoloring algorithm. The numerical costs for solving Eq. (2) depend linearly on the number of GLS functions. The initial separation between grains belonging to the same GLS function must be chosen small enough to limit the computation time and sufficiently high to avoid a numerical coalescence (the grains belonging to the same GLS function can no longer be distinguished if they meet each other). To address this issue, an efficient grain recoloring algorithm has been recently developed [11] in order to handle dynamically the distribution of the grains inside the GLS functions. This methodology is composed of two major steps: (i) the separation of the connected components on the FE mesh and (ii) the swapping algorithm which detects the risk of coalescence and reassigns the grains in other GLS functions if needed.

Mesh adaptation. The model works in 2D and in 3D. Realistic predictions necessitate a sharp description of the interfaces. This issue is achieved thanks to an anisotropic mesh adaptation around

the interfaces (figure 1). As the interface moves, periodic remeshing is performed such that the refinement zone always coincides with the interface position. This technique allows improving precision and reducing computation times.
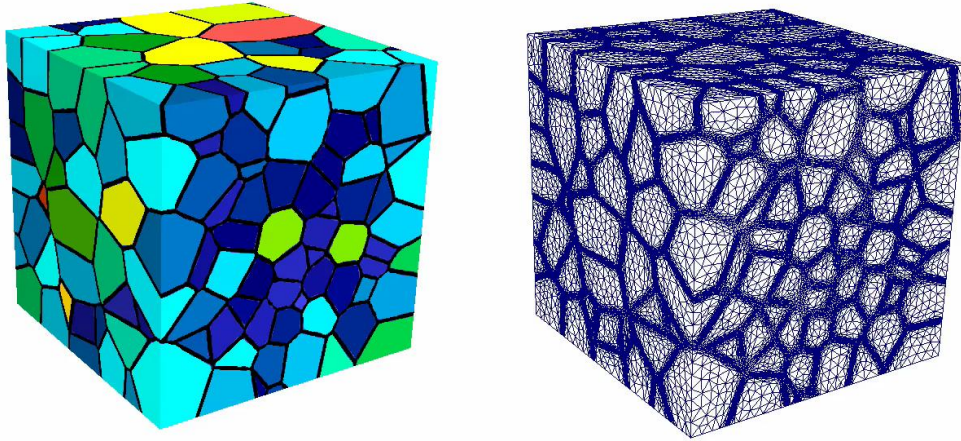

Figure 1. Polycrystal description in 3D with the used finite element mesh (anisotropic meshing near grain boundaries).

Large-scale simulations

Generation of the initial polycrystal. Simulations are performed on a Representative Volume Element (RVE) at the mesoscopic scale where the microstructural features are explicitly represented. The polycrystal is constructed respecting the topological characteristics of the grains and the metallurgical properties. The RVE can be generated from a pure experimental description (by using experimental micrographs for example) or from a statistical method. For the latter, efficient high density packing algorithms have been developed to respect a given grain size distribution [12] (see figure 2). Boundary conditions applied to the RVE are representative of what suffered a material point at the macroscopic scale (thermomechanical cycle of the point considered).

Different 2D and 3D large-scale simulations enabled by the new major developments described previously, and which would not have been performed in acceptable computation times before, are illustrated below.
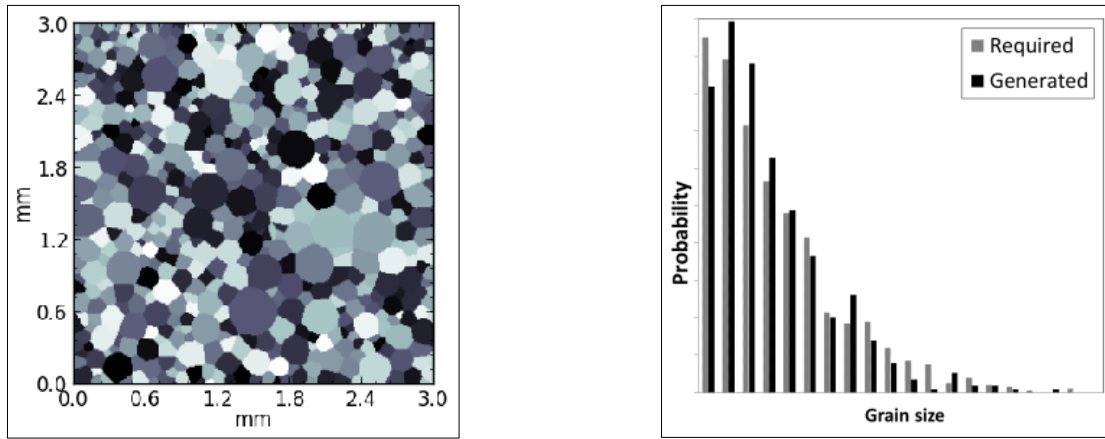
Figure 2. 2D RVE generation (500 grains) (left) respecting a given grain size distribution (right).

Pure grain growth. In case of pure grain growth, the convective term of Eq. (1) vanishes and microstructural evolution is only driven by GBs mean curvature. Figures 3 and 4 represent the microstructural evolution of a 304L austenitic stainless steel subjected to an isothermal heat treatment at 1050°C. Simulations are performed respectively on a 2D and a 3D polycrystal. In both cases, the microstructural evolution is only driven by the reduction of the total GBs length/area. With isotropic GB mobility and energy, the well-known Burke and Turnbull equation [13] is used to validate the results obtained through these full field simulations. The comparison is plotted on figure 3 showing a good agreement between both models.
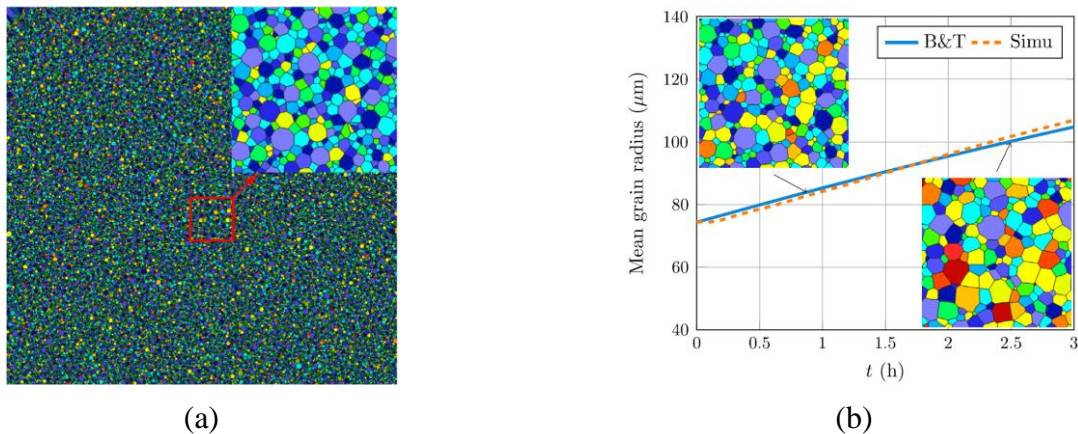

(a)

(b)

Figure 3. (a) Initial 304L 2D polycrystal (50000 grains); (b) Microstructural evolution during an isothermal heat treatment (1050°C): comparison with the Burke and Turnbull model [11, 13].
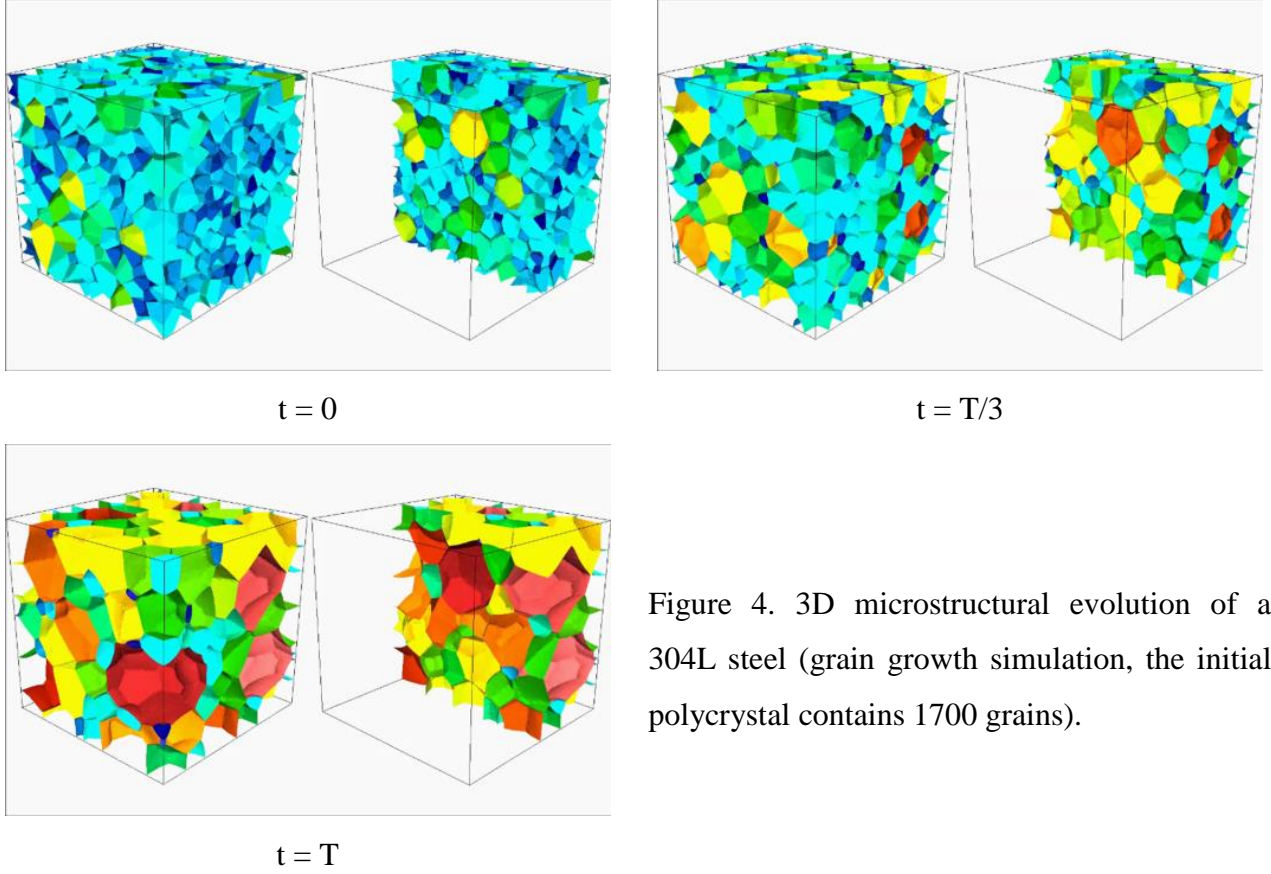
t = 0

t = T/3

t = T

Figure 4. 3D microstructural evolution of a 304L steel (grain growth simulation, the initial polycrystal contains 1700 grains).

Smith-Zener pinning (SZP) phenomenon. In order to limit the final grain size which can be detrimental for the mechanical properties, a classical method consists in precipitating second phase particles (SPP). These particles hinder the grain boundaries (GB) motion thanks to the dragging force exerted on GBs. The LS method is particularly interesting for the modeling of SZP [14] since no assumption is required concerning the shape or the dragging force exerted by the SPP. The interaction angle α between the GB and a precipitate is dictated by the balance of the surface tensions according to $\sin \alpha = \left(\gamma_2^p - \gamma_1^p \right)/\gamma$, where γ_1^p, γ_2^p and γ are respectively the surface tensions associated with the interfaces Γ_1^p, Γ_2^p and Γ_{12} (figure 5(a)). This constraint can be simply imposed by the mean of a boundary condition in the considered LS framework:

$$\frac{\nabla \psi}{\|\nabla \psi\|} . \vec{n} = \nabla \psi . \vec{n} = \sin \alpha. \tag{3}$$

When a GB passes through a particle, its shape thus adapts to satisfy Eq. (3), which modifies its local curvature and therefore its kinetic. If this approach is usually efficient, under specific conditions, abnormal grain growth (AGG) may occur. AGG can be described as the selective growth of only a few grains while other grains do not grow in the microstructure. It may occur as a result of a heterogeneous stored energy field leading to a driving force for some grain boundaries that overcomes the SZP force, or as a result of GB energy anisotropy, or as a result of a

heterogeneous SPP distribution. The development of efficient and accurate modelling tools able to account for the SZP phenomenon is thus necessary.

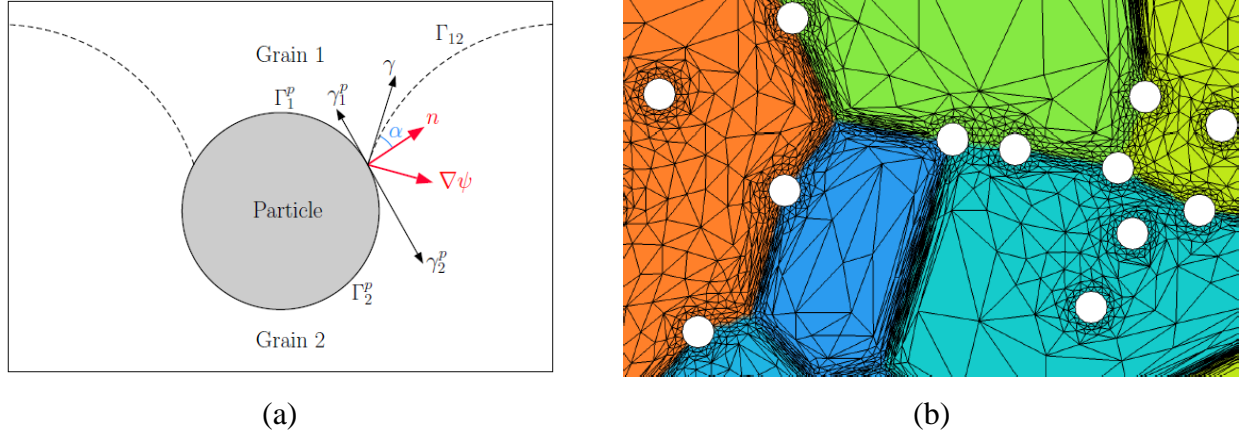(a)   (b)

Figure 5. (a) Scheme illustrating the SPP/GB interaction; (b) View of a FE mesh used for the Zener pinning simulations. The voids in the mesh (white disks) represent the SPP [15].

Based on the work described in [9], the recent numerical developments [10, 11] allowed performing 2D and 3D simulations as shown in figures 6 and 7. SPP are considered inert and are represented as holes in the FE mesh (white disks in figures 5(b) and 6(a) and green surfaces in figure 7) [15]. In such a way, incoherent or coherent particle/grain interfaces can be considered through appropriate boundary conditions and the dragging effect is naturally modelled by the modification of the local curvature when the GB passes through the particles.

Figure 6 shows an example of 2D simulations performed with the DIGIMU$^{®}$ software. An isothermal treatment at 985°C during 30min is applied on an Inconel® 718 superalloy. At this temperature, the alloy contains δ precipitates at thermodynamic equilibrium, considered as SPP in the simulation. A two-dimensional RVE composed of 800 grains of γ phase is generated with a mean grain size of 8μm (figure 6(a)). 1% surface fraction of δ phase is considered with a mean particle size of 400nm. The mean grain size evolution during the isothermal treatment is plotted figure 6(b). In order to evaluate the strong dragging effect exerted by SPP on GBs, results of a similar simulation without adding SPP in the RVE are also plotted.
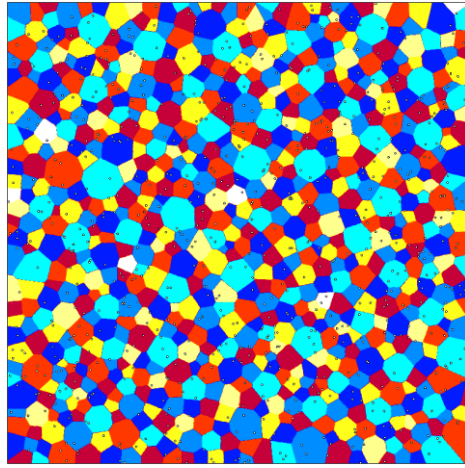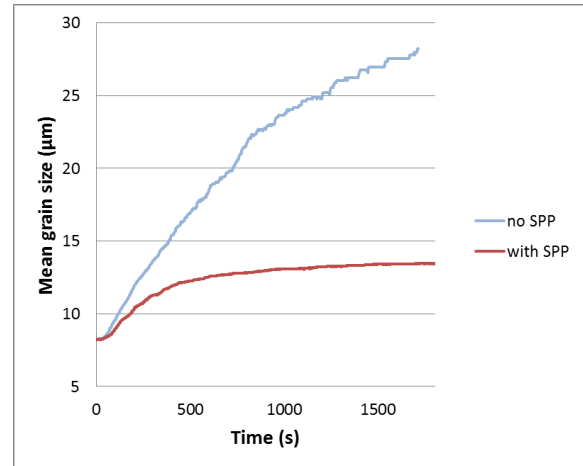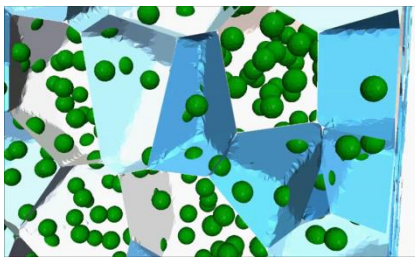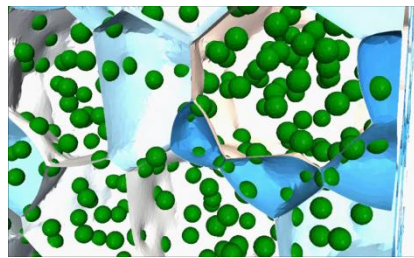
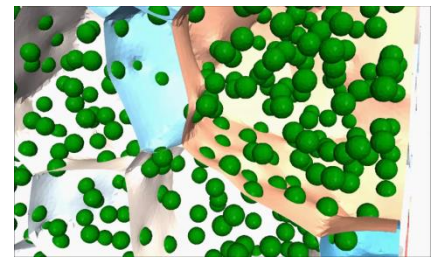(a)   (b)

Figure 6. (a) 2D RVE composed of 800 grains (mean grain size of 8µm) and 1% surface fraction SPP (mean particles radius of 400nm); (b) grain size evolution with and without SPP considering an Inconel® 718 alloy held at 985°C during 30min calculated by the DIGIMU® software.

t=0   t=T/8   t=T

Figure 7. A 3D grain growth simulation for Inconel® 718. The green spheres represent the precipitates.

The full field approach described here has also been applied to the modelling of recrystallization [16]. In that case, the driving force for grain boundaries motion is given by both grain boundaries mean curvature and stored energy gradients between neighbouring grains (recrystallized or non-recrystallized). Preferential sites for nucleation of newly recrystallized grains can also be controlled by a suitable choice of nucleation criteria (topological and/or stored energy based).

Conclusion

A full field approach using the level set method in a finite element context has been used to simulate the microstructural evolution during thermal treatments. Modelling at the mesoscopic scale can be a help for understanding complex microstructural phenomena but it can also be used to optimize/calibrate higher scale models (like mean field models). These simulations allow describing in a natural way the materials in terms of microstructural features. The recent improvements done to reduce the high computation times generally associated with these models make possible now their use for industrial applications though the DIGIMU® software.

References

[1] P. Bernard, S. Bag, K. Huang, R.E. Logé, Mat. Sci. Eng. A 528 (2011) 7357-7367.

[2] M. Mukherjee, U. Prahl, W. Bleck, Steel Res. Int. 81 (2010) 1102-1116.

[3] A.D. Rollett, D. Raabe, Comp. Mater. Sci. 21 (2001) 69-78.

[4] K. Piekos, J. Tarasiuk, K. Wierzbanowski, B. Bacroix, Recrystallization and Grain Growth III Proc. (Jeju Island, Korea) (2007) 1157-1162.

[5] L.Q. Chen, Ann. Rev. Mater. Res. 32 (2002) 113-140.

[6] M. Bernacki, H. Resk, T. Coupez, R.E. Logé, Mod. Sim. Mat. Sci. Eng. 17 (2009).

[7] M. Bernacki, R.E. Logé, T. Coupez, Scr. Mat. 64 (2011) 525-528.

[8] A.L. Cruz-Fabiano, R. Logé, M. Bernacki. Comp. Mat. Sci. 92 (2014) 305–312.

[9] A. Agnoli, N. Bozzolo, R.E. Logé, J.-M. Franchet, J. Laigo, M. Bernacki, Comp. Mat. Sci. 89 (2014) 233-241.

[10] M. Shakoor, B. Scholtes, P.-O. Bouchard, M. Bernacki, App. Math. Mod. 39 (2015) 7291-7302.

[11] B. Scholtes, M. Shakoor, A. Settefrati, P.-O. Bouchard, N. Bozzolo, M. Bernacki, Comp. Mat. Sci. 109 (2015) 388-398.

[12] K. Hitti, P. Laure, T. Coupez, L. Silva, M. Bernacki, Comp. Mat. Sci., 61 (2012) 224–238.

[13] J.E. Burke, D. Turnbull, Prog. in Met. Phys., 3 (1952) 220-292.

[14] C. Zener, C.S. Smith, Trans. AIME 175, 15 (1948).

[15] B. Scholtes, D. Ilin, A. Settefrati, N. Bozzolo, A. Agnoli, M. Bernacki, Superalloys 2016: Proceedings of the 13th International Symposium on Superalloys, TMS, 2016.

[16] B. Scholtes, R. Boulais-Sinou, A. Settefrati, D. Pino Muñoz, I. Poitrault, A. Montouchet, N. Bozzolo, and M. Bernacki, Computational Materials Science, 122 (2016) 57-71.